[40]R. J. Baxter (unpublished).

[41]J. D. Johnson, S. Krinsky, and B. M. McCoy, Phys. Rev. Lett. 29, 492 (1972).

[42]B. I. Halperin and P. C. Hohenberg, Phys. Rev. Lett. 19, 700 (1967); Phys. Rev. Lett. 19, 940 (1967).

[43]J. L. Lebowitz and L. Onsager, in *Proceedings of the Fifth International Conference on Low-Temperature Physics and Chemistry, Madison, Wisc.*, 1957, edited by J. R. Dillinger (University of Wisconsin Press, Madison, 1958), p. 119.

[44]It is also worth noting that high-temperature series expansions for the $d=3$, spin ∞, XY ($n=2$) model indicate $\nu=0.670\pm0.007$ and $\alpha=0.00\pm0.05$; see Ref. 2 and D. Jasnow and M. Wortis, Phys. Rev. 176, 739 (1968). Very similar results are found for the corresponding planar-spin ($n=2$) models, as discussed in Ref. 2; see also R. G. Bowers and G. S. Joyce, Phys. Rev. Lett. 19, 630 (1967); H. E. Stanley, Phys. Rev. Lett. 20, 589 (1968); and D. Jasnow, Ph.D. thesis (University of Illinois, 1969) (unpublished).

PHYSICAL REVIEW A VOLUME 8, NUMBER 2 AUGUST 1973

Critical Phenomena in Systems of Finite Thickness. III. Specific Heat of an Ideal Boson Film

Michael N. Barber* and Michael E. Fisher

Baker Laboratory, Cornell University, Ithaca, New York 14850

(Received 29 August 1972)

The specific heat at constant density of an ideal-Bose-fluid film of thickness $L=l\rho^{-1/3}$, but infinite lateral extent, is calculated analytically to order l^{-2}. Both hard-wall and periodic boundary conditions are considered. Good agreement with the numerical calculations of Goble and Trainor for the total specific heat under hard-wall conditions is obtained down to $l\simeq10$. In the critical region, the large-l behavior accords with the scaling theory of finite-size effects. The appropriate scaling functions and the surface specific heat are explicitly calculated.

I. INTRODUCTION AND SUMMARY

Recent analytical calculations[1] on the spherical model[2] have given considerable support to the scaling theory[3,4] of finite-size effects in the critical region. This theory appears also to predict correctly the effects of finite size and surfaces on the critical behavior of more realistic models (see Refs. 3 and 4 for a more complete discussion including various qualifications and a review of the existing calculations).

It is well known that an ideal Bose gas in three dimensions exhibits a phase transition with a sharp critical temperature[5]; the correspondence with other critical phenomena has been discussed, in detail, by Gunton and Buckingham.[6] Moreover, like the spherical model, the ideal Bose gas is mathematically tractable in all dimensions. Hence the effects of finite size and surfaces on its critical behavior may be investigated analytically,[7] and compared in detail with the scaling predictions. Although the spherical model and the ideal Bose gas are effectively equivalent in the immediate critical region[6] there are sufficient differences, both in mathematical detail and physical application, that separate discussions are illuminating. Thus the ideal Bose transition provides a model, albeit a rather crude one, of the superfluid transition in real helium; in particular, ideal Bose films are of interest in connection with real helium films. Indeed, many authors[8-11] have studied ideal Bose films and other finite geometries. For the most part, however, the previous calculations do not reveal clearly (or at all) the nature of the asymptotic behavior for large thickness L nor provide very explicit expressions for the finite-thickness thermodynamic properties. (There has also been a tendency to attempt to identify particular "condensation," "transition," or "onset" points rather than recognizing fully the absence of a sharp transition in any finite geometry, and acknowledging the consequent "rounding" and distortion of all properties.)

In this paper we aim to give a detailed discussion of the specific heat $C_V^\tau(T, l)$, at constant number density ρ (or constant volume) of a two-dimensional ideal boson film of thickness $L=l\rho^{-1/3}$, and infinite lateral extent. We consider both standard hard-wall boundary conditions (denoted by superscript $\tau=1$) and periodic boundary conditions applied across the film (denoted by $\tau=0$). The calculations extend, and specialize, an earlier analysis[4,7] of the shift and rounding of the transition as a function of l in a d'-dimensional ideal Bose "film" which is infinite in $d'=d-1$ dimensions but of finite thickness L in the dth dimension.

To summarize our results, recall[5,6] that the bulk specific heat of an ideal Bose fluid in an infinite three-dimensional domain remains finite at the critical point $T = T_c$ with value

$$C_V(T_c)/\rho k_B = \tfrac{15}{4}\zeta(2\tfrac{1}{2})/\zeta(1\tfrac{1}{2}) = 1.925\,672\ldots\ , \qquad (1.1)$$

where, here and below, C_V denotes the heat capacity per unit *volume*. However, $C_V(T)$ has a sharp pointed maximum or "kink" at T_c where the derivative

$$C_V'(T) = \frac{dC_V(T)}{dT} \qquad (1.2)$$

has a discontinuity given by

$$T_c \Delta C_V'/\rho k_B = T_c \lim_{\epsilon\to 0}[C_p'(T_c - \epsilon) - C_p'(T_c + \epsilon)]/\rho k_B$$
$$= 27[\zeta(1\tfrac{1}{2})]^2/16\pi = 3.665\,769\ldots\ . \qquad (1.3)$$

In these expressions $\zeta(z)$ is, as usual, the Riemann ζ function.

On the other hand, for a film of finite thickness there is no true transition and we expect $C_V^\tau(T, l)$ to be analytic, the kink being rounded. Furthermore, the scaling theory of finite-size effects in the critical region predicts[3,4] that the singular part of $C_V^\tau(T, l)$ in the critical region depends only on the scaled variable $z \propto L/\xi(T)$, where $\xi(T)$ is the bulk correlation length. This, of course, diverges at the bulk critical temperature T_c according to[3]

$$\xi(T) \sim (T - T_c)^{-\nu}, \quad T \to T_c + . \qquad (1.4)$$

Since for an ideal Bose fluid in three dimensions we have[6] $\nu = 1$, scaling theory leads to the form[3,4]

$$T_c \frac{\partial C_V^\tau(T, l)}{\partial T} \approx \rho k_B Y^\tau(l\dot{t})\ , \quad l \to \infty\ , \quad T \to T_c\ . \qquad (1.5)$$

In this expression allowance is made for an effective displacement[3,4,7] $\epsilon(l)$ of the critical temperature through the introduction of the shifted temperature variable

$$\dot{t} = t + \epsilon(l)\, , \qquad (1.6)$$

where, as usual, the reduced temperature deviation is

$$t = (T - T_c)/T_c\ . \qquad (1.7)$$

To recover the bulk behavior (1.3) in the limit $l \to \infty$ the scaling functions $Y^\tau(x)$ should satisfy

$$\lim_{x\to\infty} \{Y^\tau(-x) - Y^\tau(x)\} = 27[\zeta(1\tfrac{1}{2})]^2/16\pi\ . \qquad (1.8)$$

These expectations are indeed borne out by the analysis we present in the following sections. In particular, the appropriate scaling functions can be calculated explicitly and their properties checked.

For the case of a film confined by hard-wall boundary conditions the specific heat has been evaluated numerically for various thicknesses by Goble and Trainor.[9,10] Inspection of their numerical data reveals a striking feature; namely, the specific heat of the film is *enhanced* above the bulk value. Intuitively, one feels that the presence of hard walls should depress the specific-heat anomaly. To investigate this paradox we have calculated explicitly the surface (or wall) specific heat $C_V^\times(T)$ defined[3,4] through

$$C_V^1(T, l) \approx C_V(T) + (2/l)C_V^\times(T) + \cdots\ , \qquad (1.9)$$

as $l \to \infty$ with T fixed and unequal to T_c. Above the bulk critical temperature T_c, the surface specific heat is found to be *positive*, and hence tends to increase the over-all specific heat. Indeed, when T approaches T_c from above, $C_V^\times(T)$ diverges logarithmically. Conversely, below the transition, $C_V^\times(T)$ is negative and approaches a constant at T_c as shown in Fig. 1.

The specific heat of an ideal boson film has also been studied recently by Pathria[11] using different mathematical techniques. His final expression is valid for both $T \to T_c$ and $l \to \infty$; i.e., precisely

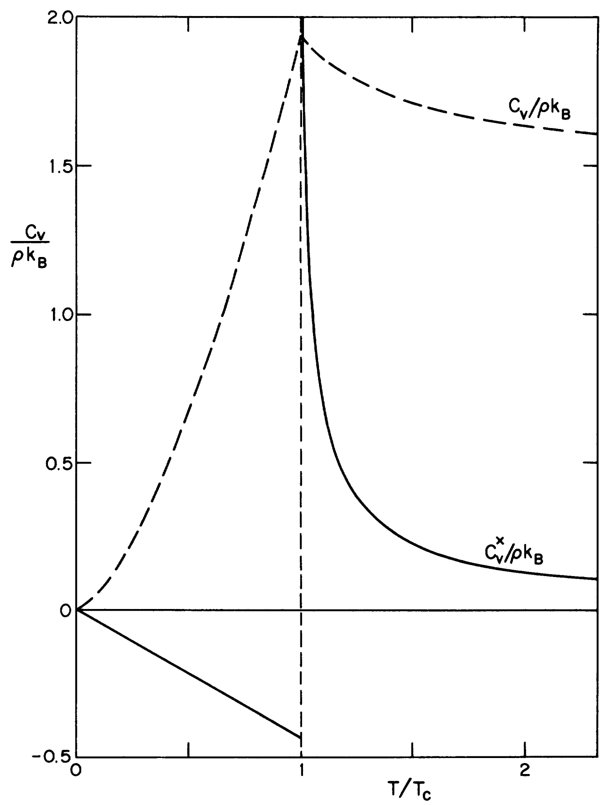

FIG. 1. Surface specific heat $C_V^\times(T)$ of a three-dimensional ideal Bose gas. For comparison, the bulk specific heat $C_V(T)$ is also shown (broken curve). Note that the units of both specific heats are such that at high temperatures $C_V/\rho k_B$ tends to $\frac{3}{2}$.

in the regime where scaling should be applicable. However, it is not obvious from his expressions whether or not $C_V^\tau(T, l)$ may be represented in a scaled form consistent with the general theory. In fact, a relatively simple scaled form does exist as we shall show in Sec. IV D.

Finally, one can test the convergence of the asymptotic expansions for large L against the numerical results of Goble and Trainor for finite L. A partial comparison by Pathria,[11] of the variation of the specific-heat maximum with thickness, suggested that the convergence was rather slow so that higher-order terms in l^{-1} would be required when $l \lesssim 50$. A crucial assumption in Pathria's analysis, however, was that the temperature $T_m(l)$ of the specific-heat maximum was close to T_c; but the ratio $(T_m - T_c)/T_c$ is not in fact small unless $l \gtrsim 60$. In Sec. IV C we show that when this assumption is relaxed, the asymptotic results, even if truncated at order l^{-1}, are in remarkably good agreement with the numerical data down to $l \simeq 10$.

Our detailed arguments are organized as follows: In Sec. II we review briefly the formulation and analysis of the free energy of an ideal boson film, within the grand canonical ensemble. The details will be available elsewhere,[7] and our aim here is only to motivate the basic results, on which the subsequent analysis is based. The surface specific heat $C_V^\times(T)$ is calculated in Sec. III, while in Sec. IV, the behavior of $C_V^\tau(T, l)$ is analyzed. Our conclusions are summarized briefly in Sec. IV E.

II. REVIEW OF BASIC RESULTS FOR IDEAL BOSON FILMS

A. Formulation

For an ideal Bose fluid in a domain Ω of volume V_Ω the thermodynamic quantities may be derived from the grand potential,[6]

$$\beta p(\mu, T) = -V_\Omega^{-1} \sum_{\vec{k}} \ln\{-\exp[-\beta(\epsilon_{\vec{k}} - \mu)]\} , \quad (2.1)$$

where $\beta = (k_B T)^{-1}$, $\epsilon_{\vec{k}}$ is the energy of the single-particle state $\vec{k}$, and the chemical potential μ is determined by the *density constraint*

$$\rho = \left(\frac{\partial p}{\partial \mu}\right)_T , \quad (2.2)$$

where ρ is the over-all number density. It is convenient to introduce the dimensionless thickness

$$n = L/\pi^{1/2}\Lambda , \quad (2.3)$$

and the reduced chemical potential

$$\phi = -\beta(\mu - \epsilon_0) \begin{cases} >0, & T > T_c \\ =0, & T < T_c \end{cases} \quad (2.4)$$

where the thermal de Broglie wavelength is

$$\Lambda = (2\pi\hbar^2/mk_B T)^{1/2} . \quad (2.5)$$

The basic expression for $p(\mu, T)$ for a two-dimensional film of thickness L and infinite lateral extent is then[7]

$$\Lambda^3 \beta p = P_3^\tau(\phi, n) = \frac{1}{n\pi^{1/2}} \sum_{r\in\mathcal{L}_\tau} F_2[\phi + \tfrac{1}{4}n^{-2}(r^2 - r_{0,\tau}^2)] , \quad (2.6)$$

where the so-called Bose functions[12,13] are defined by

$$F_\sigma(z) = \sum_{n=1}^{\infty} n^{-\sigma} e^{-nz} . \quad (2.7)$$

The sum in (2.6) runs over a subset $\mathcal{L}_\tau$ of the integers with

$$r_{0,\tau} = \min\{|r| ; r \in \mathcal{L}_\tau\} . \quad (2.8)$$

For the boundary conditions of interest, namely,

($\tau = 0$) periodic, i.e., $\psi(x) = \psi(x + L)$,

and

($\tau = 1$) free surfaces with $\psi(0) = \psi(L) = 0$,

where $\psi(x)$ is a single-particle wave function, the appropriate subsets are[7]

$$\mathcal{L}_0 = (0, 1, 2, \pm 4, \ldots, \pm\infty), \qquad \mathcal{L}_1 = (1, 2, 3, \ldots, +\infty) . \quad (2.9)$$

B. Analysis of $P_3^\tau(\phi, n)$ for large n

For periodic boundary conditions we can obtain an expression for

$$P_3^0(\phi, n) = \frac{\pi^{-1/2}}{n} \sum_{r=-\infty}^{+\infty} F_2\left(\phi + \frac{r^2}{n^2}\right) , \quad (2.10)$$

in the limit $n \to \infty$, by noting that $F_2(z)$ has the expansion[12,13]

$$F_2(z) = \tfrac{1}{6}\pi^2 + z \ln z - z + \sum_{n=2}^{\infty} (-z)^n \frac{\zeta(2-n)}{n!} , \quad (2.11)$$

valid for $|z| < 2\pi$ and $|\arg z| < \pi$. For constant $\phi > 0$, or equivalently fixed $T > T_c$, the summand $F_2(\phi + y^2)$ of (2.10) is thus an analytic function of y in the strip

$$|\mathrm{Im}\, y| < \phi^{1/2} . \quad (2.12)$$

Consequently, $P_3^0(\phi, n)$ will approach its limit,

$$\lim_{n\to\infty} P_3^0(\phi, n) = \pi^{-1/2} \int_{-\infty}^{\infty} F_2(\phi + y^2)\, dy = F_{5/2}(\phi) , \quad (2.13)$$

exponentially fast in n when $\phi > 0$. Specifically, we find[7]

$$P_3^0(\phi, n) \approx F_{5/2}(\phi) + 2\pi^{-1/2}\phi^{1/2} e^{-2\pi n\sqrt{\phi}}/n^2 , \qquad n \to \infty , \quad \phi > 0 . \quad (2.14)$$

However, near T_c, when ϕ is small, the convergence will be slow, and there exists[7] an n-dependent scaling of ϕ, namely,

$$x=\phi n^2=-2\mu L^2 m/h^2 \quad , \tag{2.15}$$

for which the asymptotic behavior is distinct from that at constant ϕ. A detailed analysis[7] shows that in this scaled critical region the required expansion of (2.6) is

$$P_3^0(x/n^2, n)=\zeta(2\tfrac{1}{2})-x\zeta(1\tfrac{1}{2})/n^2+\pi^{-1/2}H_3^0(x)/n^3 + O(n^{-4}) \quad , \tag{2.16}$$

where

$$H_3^0(x)=2R_{2,0}(x)-x[1-\ln(4\pi^2 x)]+\zeta(3)/\pi^2 \quad , \tag{2.17}$$

in which the remnant function,[14] of order (2, 0), is defined by

$$R_{2,0}(x)=\sum_{r=1}^{\infty}\{(r^2+x)\ln[1+(x/r^2)]-r^2\} \quad . \tag{2.18}$$

Tables and analytic and asymptotic expansions for the general remnant function $R_{\sigma\tau}(x)$ have recently been obtained.[14]

For hard-wall boundary conditions, there are again two similar regimes of distinct asymptotic behavior. In this case (2.6) may be written, using (2.9), as

$$P_3^1(\phi, n)=\frac{\pi^{-1/2}}{n}\sum_{r=1}^{\infty}F_2\left(\phi+\frac{r^2}{4n^2}-\frac{1}{4n^2}\right) \cdot \tag{2.19}$$

For constant $\phi>0$, i.e., fixed $T>T_c$, we may, to order n^{-1}, neglect the small term $\frac{1}{4}n^{-2}$ in the argument of F_2. On converting the sum to an integral, for large n we then obtain

$$P_3^1(\phi, n)=F_{5/2}(\phi)-\tfrac{1}{2}F_2(\phi)/n\pi^{1/2}+O(n^{-2}) \quad . \tag{2.20}$$

Note the occurrence of a definite surface contribution of order n^{-1}. However, as emphasized by Fisher[3] such an expansion is valid only away from T_c. In the critical region, specified again via (2.15), it must break down, and we find[7] instead

$$P_3^1(x/n^2, n)=\zeta(2\tfrac{1}{2})-\pi^{3/2}/12n+(\tfrac{1}{4}-x)\zeta(1\tfrac{1}{2})/n^2 + \pi^{-1/2}(x-\tfrac{1}{4})\ln n/n^3+\pi^{-1/2}H_3^1(x)/n^3 + O(n^{-4}) \quad , \tag{2.21}$$

where, utilizing the remnant function again,

$$H_3^1(x)=\tfrac{1}{4}R_{2,0}(4x-1)+(x-\tfrac{1}{4})\ln(4\pi)+\zeta(3)/8\pi^2 \quad . \tag{2.22}$$

These results suffice for discussing the specific heat of a thick film. In Sec. III we derive, from (2.20), an expression for the surface specific heat, while in Sec. IV, (2.16) and (2.21) will be used to establish the scaling representation for the specific heat in the central region. Although $n=L/\Lambda\pi^{1/2}$ is a convenient parameter for the formal asymptotic expansion of $P_3^\tau(\phi, n)$, it is a somewhat unphysical length parameter since it depends on T. A more natural and conventional choice, which will be employed below, is

$$l=L\rho^{1/3}=n\pi^{1/2}[\zeta(1\tfrac{1}{2})]^{1/3}(T/T_c)^{-1/2} = L[\zeta(1\tfrac{1}{2})]^{1/3}/\Lambda_c \quad , \tag{2.23}$$

which is proportional to the mean interparticle spacing.

III. SURFACE SPECIFIC HEAT

In this section we calculate the surface specific heat $C_V^\times(T)$, defined by (1.9). For $T>T_c$, we have from (2.20), on introducing (2.23),

$$\Lambda_c^3\beta_c p=(T/T_c)^{5/2}F_{5/2}(\phi)-\tfrac{1}{2}\alpha(T/T_c)^2F_2(\phi)/l+O(l^{-2}), \tag{3.1}$$

where the subscript c denotes a quantity evaluated at $T=T_c$, and, for convenience, we have written

$$\alpha=[\zeta(1\tfrac{1}{2})]^{1/3}=1.377\,247\ldots \quad . \tag{3.2}$$

The reduced chemical potential ϕ is determined by the density constraint (2.2), which may be written

$$\rho=-\frac{\partial(\beta p)}{\partial\phi} . \tag{3.3}$$

From the definition (2.7) we find

$$\frac{d}{dz}F_\sigma(z)=-F_{\sigma-1}(z) \quad , \tag{3.4}$$

so that in (3.1) ϕ is determined by

$$\Lambda_c^3 p=(T/T_c)^{3/2}F_{3/2}(\phi)-\tfrac{1}{2}\alpha(T/T_c)F_1(\phi)/l+O(l^{-2}) \quad . \tag{3.5}$$

The remaining thermodynamic quantities follow by the standard relations. In particular, the entropy density is given by

$$S(T)=\left(\frac{\partial p}{\partial T}\right)_\mu=\left(\frac{\partial p}{\partial T}\right)_\phi+\left(\frac{\partial p}{\partial\phi}\right)_T\left(\frac{\partial\phi}{\partial T}\right)_\mu = \left(\frac{\partial p}{\partial T}\right)_\phi-\frac{\phi}{T}\left(\frac{\partial p}{\partial\phi}\right)_T \quad , \tag{3.6}$$

where we should note that all derivatives are to be taken at constant L or, by (2.23), constant l, while $\phi=-\beta(\mu-\epsilon_0^\tau)$ and ϵ_0^τ depends only on L. Hence on differentiating (3.1), we find

$$\Lambda_c^3 S/k_B=\tfrac{1}{2}(T/T_c)^{3/2}[5F_{5/1}(\phi)+2\phi F_{3/2}(\phi)] - \alpha(T/T_c)[F_2(\phi)+\tfrac{1}{2}\phi F_1(\phi)]/l+O(l^{-2}) \quad . \tag{3.7}$$

It is convenient at this stage to write

$$\phi = \phi_0 + \phi' \ , \tag{3.8}$$

where ϕ_0 is determined by the bulk constraint

$$\Lambda_c^3 \rho = (T/T_c)^{3/2} F_{3/2}(\phi_0) = \zeta(1\tfrac{1}{2}) \ . \tag{3.9}$$

On substituting (3.8) in (3.5) and expanding about ϕ_0, which is positive for $T > T_c$, we find

$$\phi' = -\tfrac{1}{2}\alpha l^{-1}(T_c/T)^{1/2} F_1(\phi_0)/F_{1/2}(\phi_0) + O(l^{-2}) \ . \tag{3.10}$$

Similarly we may expand (3.7) about ϕ_0 to obtain

$$\Lambda_c^3 S/k_B = \tfrac{1}{2}(T/T_c)^{3/2}(5F_{5/2} + 2\phi_0 F_{3/2}) - \alpha(T/T_c) l^{-1}[F_2 - \tfrac{3}{4}(F_{3/2}F_1/F_{1/2})] + O(l^{-2}) \ , \tag{3.11}$$

where we have adopted the convention[5]

$$F_\sigma = F_\sigma(\phi_0) \ . \tag{3.12}$$

The first term in (3.11) represents simply the entropy density of a bulk three-dimensional ideal Bose fluid. The second term yields the surface entropy density, which we write explicitly as

$$S^\times(T)/k_B = \tfrac{1}{4}(\alpha/\Lambda_c^3)(T/T_c)\Omega(\phi_0) \ , \tag{3.13}$$

where, recalling that there are two free surfaces,

$$\Omega(\phi_0) = 3(F_{3/2}F_1/2F_{1/2}) - 2F_2 \tag{3.14}$$

and α is defined in (3.2). The surface specific heat is now given by

$$C_V^\times(T) = T\left(\frac{\partial S^\times}{\partial T}\right)_\rho = T\left(\frac{\partial S^\times}{\partial T}\right)_{\phi_0} + T\left(\frac{\partial S^\times}{\partial \phi_0}\right)_T \left(\frac{\partial \phi_0}{\partial T}\right)_\rho , \tag{3.15}$$

which, by (3.13), yields

$$\Lambda_c^3 C_V^\times/k_B = \tfrac{1}{4}\alpha(T/T_c)\Sigma(\phi_0) \ , \tag{3.16}$$

$$\Sigma(\phi_0) = \Omega(\phi_0) + \Omega'(\phi_0) T\left(\frac{\partial \phi_0}{\partial T}\right)_\rho \ , \tag{3.17}$$

where the prime denotes differentiation. For $T > T_c$, the definition (3.9) yields

$$T\left(\frac{\partial \phi_0}{\partial T}\right)_\rho = 3F_{3/2}/2F_{1/2} \ , \tag{3.18}$$

and hence, using (3.17), we obtain the explicit result

$$\Sigma(\phi_0) = 9(F_{3/2}/2F_{1/2})^2[(F_1 F_{-1/2}/F_{1/2}) - F_0] - 2F_2 + 9(F_{3/2}F_1/4F_{1/2}) \ , \quad T > T_c \ . \tag{3.19}$$

When $\phi_0 \to 0$, i.e., $T \to T_c+$, we have[12,13]

$$\begin{aligned} &F_\sigma(\phi_0) \to \zeta(\sigma) \ , && \sigma > 1 \ , \\ &F_1(\phi_0) = -\ln\phi_0 + O(\phi_0) \ , && \\ &F_\sigma(\phi_0) = \Gamma(1-\sigma)\phi_0^{\sigma-1} + O(1) \ , && \sigma < 1 \ . \end{aligned} \tag{3.20}$$

Hence for small ϕ_0 the behavior is

$$\Sigma(\phi_0) \approx -9[\zeta(1\tfrac{1}{2})]^2(\ln\phi_0)/8\pi + O(1) \ , \tag{3.21}$$

while from (3.18) we find

$$\phi_0 \approx 9t^2/16\pi \quad (T \to T_c+) , \tag{3.22}$$

t being defined in (1.7). It follows that the surface specific heat *diverges logarithmically* according to

$$C_V^\times(T)/\rho k_B \simeq (9/16\pi)[\zeta(1\tfrac{1}{2})]^{4/3}\ln(t^{-1}) + O(1) \ . \tag{3.23}$$

Furthermore, since the prefactor is positive the total heat capacity of a finite-thickness film will be enhanced over the corresponding bulk heat capacity. As noted in Sec. I this effect might have been anticipated from the numerical results of Goble and Trainor.[9,10]

To obtain an expression for $C_V^\times(T)$ beneath the transition, we recall [see (2.4)] that

$$\phi_0 \equiv 0 \quad \text{for} \quad T \leqslant T_c \ . \tag{3.24}$$

It follows that (3.17) and (3.14) reduce to

$$\Sigma(0) = \Omega(0) = -2\zeta(2) = -\tfrac{1}{3}\pi^2 \ , \tag{3.25}$$

which, on substitution in (3.16), yields the rather simple result

$$C_V^\times(T)/\rho k_B = -\tfrac{1}{12}\pi^2[\zeta(1\tfrac{1}{2})]^{-2/3}(T/T_c) \ , \quad T \leqslant T_c \ . \tag{3.26}$$

Note that in this case the surface specific heat is negative and approaches a constant as $T \to T_c-$. This result and (3.16) with (3.19) provide expressions for $C_V^\times(T)$ valid at all temperatures. The behavior is plotted for $0 \leqslant T/T_c \lesssim 2.5$ in Fig. 1, where, for comparison, the bulk specific heat $C_V(T) = C_V(T, \infty)$ is also shown.[5]

This completes our analysis of the surface or wall specific heat for a three-dimensional ideal Bose fluid. If we had considered a film with periodic boundary conditions no surface or $1/l$ contributions would have been found. Rather, from (2.14) the correction terms to the bulk behavior would decay exponentially with L [see also (4.70) below].

IV. SPECIFIC HEAT IN CRITICAL REGION

We now discuss the behavior of the specific heat $C_V^\tau(T, l)$ for a film of thickness L $(= l\rho^{-1/3})$, in the critical region. In this regime the grand potential is given in terms of the scaled variable x $(= \phi n^2)$, by (2.16) and (2.21). On introducing (2.28) these results may be written for periodic conditions $(\tau = 0)$ as

$$\Lambda_c^3 \beta_c p = \zeta(2\tfrac{1}{2})(T/T_c)^{5/2} - x\pi\alpha^5(T/T_c)^{3/2}l^{-2} + \pi\alpha^3 H_3^0(x)(T/T_c)l^{-3} + O(l^{-4}) \ , \tag{4.1}$$

and for hard-wall conditions ($\tau = 1$) as

$$\Lambda_c^3 \beta_c p = \zeta(2\tfrac{1}{2})(T/T_c)^{5/2} - \tfrac{1}{2}\zeta(2)\alpha(T/T_c)^2 l^{-1} + (\tfrac{1}{4} - x)\alpha^5 \pi (T/T_c)^{3/2} l^{-2} + \pi\alpha^3(x - \tfrac{1}{4})(T/T_c) l^{-3}[\ln l + \tfrac{1}{2}\ln(t/\pi\alpha^2)] + \pi\alpha^3 H_3^1(x)(T/T_c) l^{-3} + O(l^{-4}) \quad . \qquad (4.2)$$

The thermodynamic properties again follow by the standard relations. We consider the periodic case first as it is simpler.

A. Periodic Boundary Conditions

From (4.1) the entropy density

$$S = \left(\frac{\partial p}{\partial T}\right)_\mu = \left(\frac{\partial p}{\partial T}\right)_x \qquad (4.3)$$

is given by

$$\Lambda_c^3 S/k_B = \tfrac{5}{2}\zeta(2\tfrac{1}{2})(T/T_c)^{3/2} - \tfrac{3}{2}x\pi\alpha^5(T/T_c)^{1/2} l^{-2} + \pi\alpha^3 H_3^0(x) l^{-3} + O(l^{-4}) \quad . \qquad (4.4)$$

To obtain the specific heat under the constraint of constant density we require the temperature dependence of x which follows from (2.2), which now becomes

$$\rho = -(l^2/\pi\alpha^2)(T/T_c)\left(\frac{\partial \beta p}{\partial x}\right)_T \quad . \qquad (4.5)$$

On differentiating (4.1) this may be written

$$\Lambda_c^3 \rho = \alpha^3 = \alpha^3 (T/T_c)^{3/2} - \alpha(T/T_c) l^{-1} H_3^{0\prime}(x) + O(l^{-2}) , \qquad (4.6)$$

where, by using[14]

$$\left(\frac{d}{dx}\right) R_{2,0}(x) = R_{1,0}(x) = \ln[\sinh(\pi x^{1/2})/\pi x^{1/2}] \quad , \qquad (4.7)$$

we find

$$H_3^{0\prime}(x) = \left(\frac{d}{dx}\right) H_3^0(x) = 2\ln[2\sinh(\pi x^{1/2})] \quad . \qquad (4.8)$$

It is convenient to introduce the reduced temperature variable

$$\theta = l\alpha^2[(T/T_c)^{1/2} - (T/T_c)^{-1}] \quad ; \qquad (4.9)$$

then combining (4.6) and (4.8) yields

$$x = W_0(\theta) + O(l^{-1}) \quad , \qquad (4.10)$$

with

$$W_0(\theta) = \pi^{-2}[\sinh^{-1}(\tfrac{1}{2}e^{\theta/2})]^2 . \qquad (4.11)$$

Note that while (4.1) determines the entropy (4.4), as a function of x correct to order l^{-3}, the density constraint (4.10) is valid only to order l^{-1}. Hence when we eliminate x in favor of θ, the resulting expression for the entropy will be correct only to order l^{-2}. The analysis of Ref. 7 may be extended easily, however, to give the density constraint correct to order l^{-2}; this yields

$$x = W_0[\theta - x\pi\alpha\zeta(\tfrac{1}{2})/l] + O(l^{-2}) \quad , \qquad (4.12)$$

in place of (4.10). Iterating this relation gives

$$x = W_0(\theta) - \pi\alpha\zeta(\tfrac{1}{2}) W_0(\theta) W_0'(\theta)/l + O(l^{-2}) \quad , \qquad (4.13)$$

where from (4.11),

$$W_0'(\theta) = \left(\frac{d}{d\theta}\right) W_0(\theta) = \pi^{-2}(1 + 4e^{-\theta})^{-1/2}\sinh^{-1}(\tfrac{1}{2}e^{\theta/2}) . \qquad (4.14)$$

On substituting this expression in (4.4), differentiating with respect to T, and noting that

$$T_c\left(\frac{d\theta}{dT}\right) = \tfrac{1}{2}\alpha^2 l[2 + (T/T_c)^{3/2}](T/T_c)^{-2} \quad , \qquad (4.15)$$

we finally obtain

$$C_V^0(T, l)/\rho k_B = [15\zeta(2\tfrac{1}{2})/4\zeta(1\tfrac{1}{2})](T/T_c)^{3/2} + \Gamma_1^0(\theta, T/T_c)/l + \Gamma_2^0(\theta, T/T_c)/l^2 + O(l^{-3}) , \qquad (4.16)$$

where

$$\Gamma_1^0(\theta, t) = -\tfrac{3}{4}\alpha^4\pi t^{-1/2}(2 + t^{3/2}) W_0'(\theta) \qquad (4.17)$$

and

$$\Gamma_2^0(\theta, t) = -\tfrac{3}{4}\alpha^2\pi t^{1/2} W_0(\theta) + \tfrac{1}{2}\alpha^2\pi t^{-1}(2 + t^{3/2}) W_0'(\theta) + \tfrac{3}{4}\alpha^5\pi^2\zeta(\tfrac{1}{2}) t^{-1}(2 + t^{3/2})\{W_0(\theta)W_0''(\theta) + [W_0'(\theta)]^2\} , \qquad (4.18)$$

where, from (4.14) we have

$$W_0''(\theta) = \tfrac{1}{2}\pi^{-2}(1 + 4e^{-\theta})^{-1} + 2\pi^{-2}e^{-\theta}(1 + 4e^{-\theta})^{-3/2}\sinh^{-1}(\tfrac{1}{2}e^{\theta/2}) \quad . \qquad (4.19)$$

Before discussing the physical significance of these results we derive the analagous expressions for hard-wall conditions.

B. Hard-Wall Boundary Conditions

Proceeding as in Sec. IV A, we obtain the entropy from (4.2) and (4.3), as

$$\Lambda_c^3 S/k_B = \tfrac{5}{2}\zeta(2\tfrac{1}{2})(T/T_c)^{3/2} - \alpha\zeta(2)(T/T_c) l^{-1} + \tfrac{3}{2}(\tfrac{1}{4} - x)\pi\alpha^5(T/T_c)^{1/2} l^{-2} + \pi\alpha^3(x - \tfrac{1}{4}) l^{-3}[\ln l + \tfrac{1}{2} + \tfrac{1}{2}\ln(t/\pi\alpha^2)] + \alpha^3\pi H_3^1(x) l^{-3} + O(l^{-4}) \quad . \qquad (4.20)$$

The density constraint (4.5) now takes the form

$$\Lambda_c^3\rho = \alpha^3 = \alpha^3(T/T_c)^{3/2} - \alpha(T/T_c) l^{-1}[\ln l + \tfrac{1}{2}\ln(T/T_c) - \tfrac{1}{2}\ln(\pi\alpha^2) + H_3^{1\prime}(x)] + O(l^{-2}) \quad , \qquad (4.21)$$

where from (2.22) and (4.8),

$$H_3^{1\prime}(x)=\frac{dH_3^1}{dx}=\ln\left(\frac{2\sinh 2\pi(x-\frac{1}{4})^{1/2}}{(x-\frac{1}{4})^{1/2}}\right) . \quad (4.22)$$

We now introduce the *shifted* temperature variable

$$\dot{\theta}=\theta-\tfrac{1}{2}\ln(T/T_c)-\ln(4l\pi^{1/2}/\alpha) , \quad (4.23)$$

where θ is still defined as in (4.9). The density constraint, (4.21), can then be written

$$\ln\left(\frac{\sinh 2\pi(x-\frac{1}{4})^{1/2}}{2\pi(x-\frac{1}{4})^{1/2}}\right)=\dot{\theta}+O(l^{-1}) . \quad (4.24)$$

Finally, this expression may be inverted to give

$$x=\tfrac{1}{4}+W_1(\dot{\theta})+O(l^{-1}) , \quad (4.25)$$

where the function $W_1(\dot{\theta})$ is defined parametrically by

$$W_1(\dot{\theta})=u^2/4\pi^2 , \quad \dot{\theta}=\ln(\sinh u/u) . \quad (4.26)$$

As in the periodic case, the basic analysis[7] may be extended to yield the terms of order l^{-1}; we find

$$x=\tfrac{1}{4}+W_1(\dot{\theta})-\pi\alpha\zeta(\tfrac{1}{2})(T/T_c)^{-1/2}W_1(\dot{\theta})W_1'(\dot{\theta})/l+O(l^{-2}) , \quad (4.27)$$

where, from (4.26),

$$W_1'(\dot{\theta})=\tfrac{1}{2}\pi^{-2}u(\coth u-u^{-1})^{-1} , \quad (4.28)$$

with $u=u(\dot{\theta})$ determined as in (4.26). Now from the definition (4.23) we have

$$T_c(d\dot{\theta}/dT)=\tfrac{1}{2}\alpha^2 l[2+(T/T_c)^{3/2}](T/T_c)^{-2}-\tfrac{1}{2}(T/T_c)^{-1} . \quad (4.29)$$

On substituting (4.27) in (4.20) and differentiating with respect to T we finally obtain the specific heat as

$$\begin{aligned}C_V^1(T,l)/\rho k_B=&[15\zeta(2\tfrac{1}{2})/4\zeta(1\tfrac{1}{2})](T/T_c)^{3/2}\\&+\Gamma_1^1(\dot{\theta},T/T_c)/l+\Gamma_2^1(\dot{\theta},T/T_c)(\ln l)/l^2\\&+\Gamma_3^1(\dot{\theta},t)/l^2+O(l^{-3}) , \end{aligned}\quad (4.30)$$

where the auxiliary functions are defined by

$$\Gamma_1^1(\dot{\theta},t)=-\tfrac{1}{6}\pi^2\alpha^{-2}t-\tfrac{3}{4}\alpha^4\pi t^{-1/2}(2+t^{3/2})W_1'(\dot{\theta}) , \quad (4.31)$$

$$\Gamma_2^1(\dot{\theta},t)=\tfrac{1}{2}\pi\alpha^2t^{-1}(2+t^{3/2})W_1'(\dot{\theta}) , \quad (4.32)$$

$$\begin{aligned}\Gamma_3^1(\dot{\theta},t)=&-\tfrac{3}{4}\alpha^2\pi t^{1/2}W_1(\dot{\theta})\\&+\tfrac{1}{2}\pi\alpha^2t^{-1}(2+t^{3/2})[1+2\dot{\theta}+\ln(16\pi t/\alpha^2)]W_1'(\dot{\theta})\\&+\tfrac{3}{4}\alpha^5\pi^2\zeta(\tfrac{1}{2})t^{-1}(2+t^{3/2})\{W_1(\dot{\theta})W_1''(\dot{\theta})\\&+[W_1'(\dot{\theta})]^2\} , \end{aligned}\quad (4.33)$$

where, from (4.28), we have

$$W_1''(\dot{\theta})=\tfrac{1}{2}\pi^{-2}(u\,\mathrm{cosech}^2u+\coth u-2u^{-1})(\coth u-u^{-1})^{-3} \quad (4.34)$$

with, as before, $u=u(\dot{\theta})$ determined by (4.26).

C. Specific-Heat Maximum

We see from the results (4.16) and (4.30), that the specific heat is, as expected, analytic near T_c for finite l; in particular, $\partial C_V^\tau/\partial T$ is continuous. However, the specific heat attains a rounded maximum of value $C_{\max}^\tau(l)$, at a temperature $T_m^\tau(l)$. Furthermore, $T_m^\tau(l)$ approaches T_c as $l\to\infty$ so that one might consider T_m^τ as a "quasicritical temperature."

Although $C_\rho^\tau(T,l)$ is given correctly to order l^{-2} by (4.15) and (4.30), it is convenient and (as we shall see) sufficient for studying the maximum to truncate these expressions at order l^{-1}. By differentiation the temperature of the maximum, $T_m^\tau(l)$, is then determined by

$$15[1+2(T_c/T_m^\tau)^{3/2}]^{-2}=\pi[\zeta(1\tfrac{1}{2})]^3W_\tau''(\Theta)+O(l^{-1}) , \quad (4.35)$$

where, from (4.9) and (4.23),

$$\begin{aligned}\Theta=&\alpha^2l[(T_m^\tau/T_c)^{1/2}-(T_m^\tau/T_c)^{-1}]\\&-\tau\ln[4l\pi^{1/2}(T_m^\tau/T_c)^{1/2}/\alpha] , \end{aligned}\quad (4.36)$$

with $\tau=0$ or 1. These coupled equations may be solved numerically for T_m^τ as a function of l. The results are shown graphically in Fig. 2. For large l we can write

$$T_m^\tau/T_c=1+\epsilon_m^\tau(l) , \quad (4.37)$$

with $\epsilon_m^\tau\ll 1$. On substituting in (4.35) and (4.36), and expanding to linear order in ϵ_m^τ, we find this quasicritical-point shift to be given by

$$\epsilon_m^\tau(l)=\tfrac{2}{3}\alpha^{-2}l^{-1}[\dot{\theta}_m^\tau+\tau\ln(4l\pi^{1/2}/\alpha)]+O(l^{-2}) , \quad (4.38)$$

where $\dot{\theta}_m^\tau$ is determined by

$$W_\tau''(\dot{\theta}_m^\tau)=\tfrac{5}{3}\pi^{-1}[\zeta(1\tfrac{1}{2})]^{-3}=0.029757\ldots . \quad (4.39)$$

Solving this equation numerically gives

$$\dot{\theta}_m^0=1.3080\ldots , \quad \dot{\theta}_m^1=-1.8112\ldots , \quad (4.40)$$

so that finally,

$$\begin{aligned}\epsilon_m^\tau(l)&=(T_m^\tau-T_c)/T_c\\&\approx a_m^0/l+O(l^{-2}) \qquad (\tau=0)\\&\approx a_m^1(\ln l)/l+b_m^1/l+O(l^{-2}) \qquad (\tau=1) , \end{aligned}\quad (4.41)$$

where

$$a_m^0=\tfrac{2}{3}\alpha^{-2}\dot{\theta}_m^0=0.4597\ldots , \quad (4.42)$$

$$a_m^1=\tfrac{2}{3}\alpha^{-2}=0.3515\ldots , \quad (4.43)$$

$$\begin{aligned}b_m^1&=\tfrac{2}{3}\alpha^{-2}[\dot{\theta}_m^1+\ln(4\pi^{1/2}/\alpha)]\\&=-0.0607\ldots . \end{aligned}\quad (4.44)$$

These asymptotic results have also been obtained recently by Pathria[11] following a different route. The variation of $T_m^\tau(l)$ with l, predicted by (4.41), is shown as the dashed curves in Fig. 2. Evidently, it departs significantly from the more accurate solution of (4.31) for $l \lesssim 60$ (which at a density of 2.0×10^{22} particles/cm^3 corresponds to $L\approx 200$ Å). However, for hard walls ($\tau=1$), the solution of (4.35) is in extremely good agreement, even for relatively small values of l, with the numerical calculations of Goble and Trainor,[9,10] which are represented by the bars in Fig. 2.

A more subtle test of the convergence of the asymptotic results is provided by the variation of the maximum

$$C_{\max}^\tau(l) = C_V^\tau(T_m^\tau, l). \qquad (4.45)$$

Under hard-wall conditions Goble and Trainor[9,10] found that $C_{\max}^1(l)$ *increased* with increasing l until an absolute maximum of

$$C_{\max}^1/\rho k_B = C_{\max}^* = 1.970 \pm 2 \qquad (4.46)$$

was reached at

$$l = l^* = 17.5 \pm 1.5 \ . \qquad (4.47)$$

For $l > l^*$ the maximum declines slowly towards $C_V(T_c)$; for all $l \gtrsim 6$, however, $C_{\max}^1$ lies above $C_{Vc}=C_V(T_c)$. It is illuminating to compare this observed numerical behavior with the asymptotic results, (4.30), truncated at various orders. The simplest approximation is to truncate (4.30) at order l^{-1}, substitute with (4.37), and expand to linear order in the effective shift ϵ_m^1. Using (4.41) and (4.40), which gives $W_1'(\mathring{\theta}_m^1) = 0.3291$, we find

$$C_{\max}^1(l) = C_{Vc}[1 + c_1^*(\ln l)/l + c_1/l] + O(l^{-2}) \ , \qquad (4.48)$$

where $C_{Vc} = C_V(T_c)$ and

$$c_1^* = \alpha^{-2} = 0.5273\ldots \ , \qquad (4.49)$$

$$c_1 = \alpha^{-2}\ln(4\pi^{1/2}/\alpha) + \Gamma_1^1(\mathring{\theta}_m^1, 1) = -1.2849 \ . \qquad (4.50)$$

This result, which confirms that found by Pathria,[11] is represented by the dashed line (for $\tau=1$) in Fig. 3. The qualitative agreement with the numerical data of Goble and Trainor is satisfactory but the quantitative agreement is poor; for example, (4.48) predicts an absolute maximum of

$$C_{\max}^* \simeq 1.9584 \qquad (4.51)$$

or

$$l = l^* \simeq 31 \ . \qquad (4.52)$$

Significant improvement is obtained if one still truncates (4.30) at order l^{-1}, but now substitutes for $T_m^1(l)$ using the full solution of (4.35) and (4.36). The results are represented by the dot-

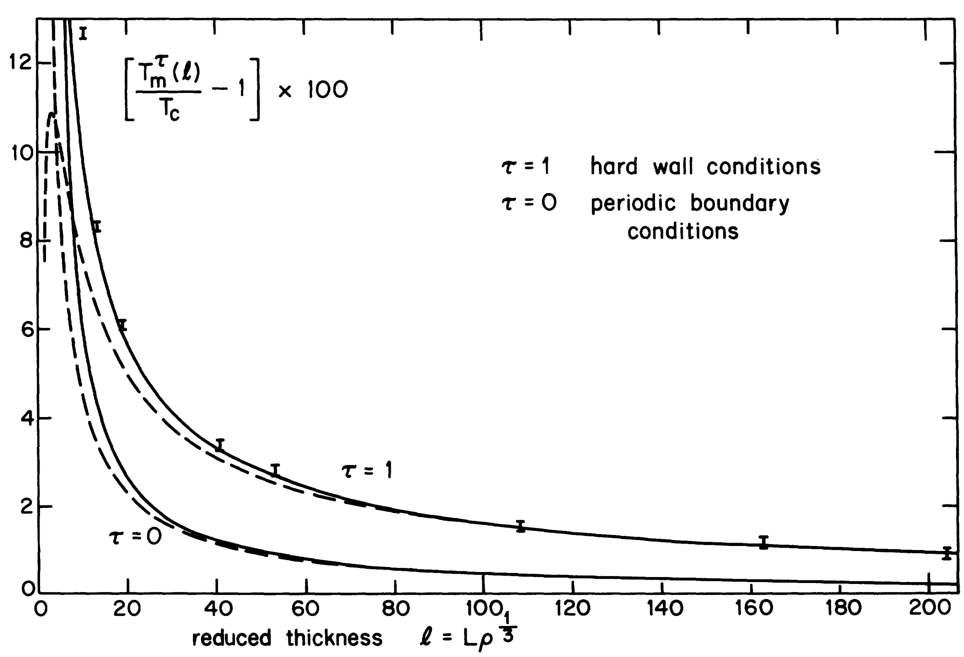

FIG. 2. Variation of the temperature $T_m^\tau(l)$ of the specific-heat maximum for a film with hard wall ($\tau=1$) and periodic ($\tau=0$) boundary conditions. The solid curves represent the solutions of (4.35), while the dashed curves represent the asymptotic expansions (4.41). The bars (*I*) denote values of $T_m^1(l)$ obtained from the numerical calculations of Goble and Trainor (Refs. 9 and 10); the error bars indicate their quoted uncertainty of ±0.1%.

dash curve in Fig. 3 and yield the improved estimates

$$C^*_{\max} \simeq 1.9626 \pm 3 \ , \tag{4.53}$$

$$l^* \simeq 27 \ . \tag{4.54}$$

To obtain higher accuracy one must retain terms of order l^{-2} in (4.30). In order to be fully consistent to this order, one should recalculate $T^1_m(l)$ from (4.35) including these extra terms. However, in view of the close agreement of the solution of (4.35) (which is exact to order l^{-1}) with the numerical calculations (see Fig. 2), the resulting changes in $T^1_m(l)$ will be small. Accordingly, one should be able to obtain a good estimate of $C^1_{\max}(l)$ by substituting the solution of (4.36) into the explicit terms in (4.30). The resulting prediction is shown by the solid line ($\tau = 1$) in Fig. 3. The agreement is remarkably good: in particular, we obtain

$$C^*_{\max} \simeq 1.9675 \pm 2 \ , \tag{4.55}$$

$$l = l^* \simeq 20 \ , \tag{4.56}$$

which compare well with the numerical estimates (4.46) and (4.47). The residual differences can probably be reduced by recalculating $T^\tau_m(l)$ to order l^{-2}. However, one should also note that for $l \gtrsim 100$, where all three asymptotic predictions essentially coincide, the numerical data appear to deviate significantly. This probably indicates that the uncertainties in the numerical estimates are somewhat greater than the $\pm 0.1\%$ quoted by Goble and Trainor.

A similar discussion is possible for periodic boundary conditions. The corresponding results are included in Fig. 3 ($\tau = 0$). The variation is less dramatic, and for $l \gtrsim 30$, well represented by

$$C^0_{\max}(l) = C_{Vc}[1 + c_0/l + O(l^{-2})] \tag{4.57}$$

with

$$c_0 = \alpha^{-2}\dot{\theta}^0_m - [3\pi\alpha^7/5\zeta(2\tfrac{1}{2})]W_0'(\mathring{\theta}^0_m) \simeq -0.1025 . \tag{4.58}$$

This is the analog of (4.48), being obtained by truncating (4.16) at order l^{-1} and expanding to first order in the shift $\epsilon^0_m(l)$. Since c_0 is negative, the specific-heat maximum for a film with periodic boundary conditions increases as l increases and always lies *beneath* the bulk value (see Fig. 3).

It is important to realize, as already noted by Krueger[8] and Pathria,[11] the absence in the periodic case, of any enhancement, or length l^*, such as found with hard walls. Goble and Trainor[10] did not

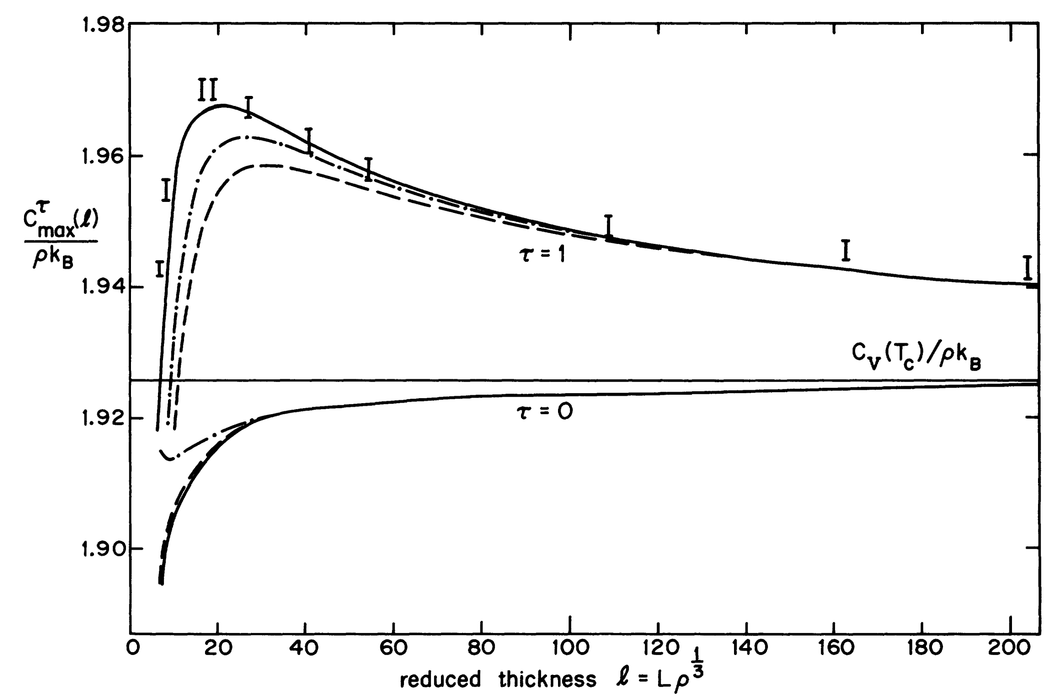

FIG. 3. Variation of the specific-heat maximum $C^\tau_{\max}(l)$ of the specific heat of an ideal Bose film with hard-wall ($\tau = 1$) and periodic ($\tau = 0$) boundary conditions. The dashed curves represent the asymptotic results (4.48) and (4.57); the dot-dash curves are derived from (4.16) and (4.30), truncated at order l^{-1}, together with $T^\tau_m(l)$ determined by solving the first-order equations (4.35) and (4.36); the solid curves represent the full second-order expressions for $C^\tau_V(T, l)$, (4.16) and (4.30), evaluated with $T^\tau_m(l)$ again determined by (4.35) and (4.36). The bars indicate values of $C^1_{\max}(l)$ obtained from the numerical calculations of Goble and Trainor (Refs. 9 and 10).

consider periodic boundary conditions: Had they done so they might not have made the rather *ad hoc* conjecture that the enhancement was a consequence of "a new statistical correlation length of about 70 Å" which distinguishes between "thick"- and "thin"-film behavior. Rather the anomalous behavior, which is connected to the unexpected sign of the surface specific heat noted in Sec. III, presumably has the same origin as the enhancement of the critical temperature, which occurs in both ideal Bose fluids and the spherical model for $d \geq 4$.[1,7] Elsewhere[1,3,7] we have argued that these anomalous features of the behavior of ideal Bose and spherical models are an indirect consequence of the constraints on the particle density (in the ideal Bose fluid) and on the mean-square spin magnitude (in the spherical model). These constraints must be imposed for all thicknesses and lead[3] to an enhancement of the off-diagonal (short-range) order and specific heat. However, the presence of hard walls at fixed chemical potential tends to depress the specific heat through the disordering effect as the wave function goes to zero at the boundaries. In a very thin film this latter effect should dominate while the first effect becomes important in thicker films. Ultimately, however, the enhanced maximum must decrease to the bulk critical value. The value $L^* = l^*\rho^{-1/3}$ then corresponds merely to the thickness at which there is an optimum balance between the effects. While in this particular sense, l^* does distinguish between "thick" and "thin" films it is hard to believe that any special significance attaches to this length. On the contrary, the range of correlation $\xi(\rho, T)$ of the off-diagonal order *does* provide a basic length scale as will become clear in Sec. IV D where the scaling properties are established. Last, it should be stressed that the marked specific-heat enhancement in the films with hard walls seems to be a rather special feature of ideal Bose fluids which is not likely to be reproduced in more realistic systems.

D. Scaling Representation

To establish a scaling representation, we recall from Sec. I that scaling is expected to apply asymptotically when $l \gg 1$, and $t = (T - T_c)/T_c \ll 1$. In terms of t, the scaled temperature variable introduced in (4.9), which is essentially $L/\xi(T)$, becomes

$$\theta = \tfrac{3}{2}\alpha^2 lt + O(lt^2) \quad . \tag{4.59}$$

Then the basic result (4.16) for periodic boundary conditions may be truncated at order l^{-1} and expressed to leading order as

$$C_V^0(T, l) = C_{Vc}[1 + l^{-1}X^0(lt) + O(l^{-2})] \quad , \tag{4.60}$$

which is valid for all $z = lt$ as $l \to \infty$ or $t \to 0$. From (4.17) and (4.14) the scaling function may be given explicitly as

$$X^0(z) = \tfrac{3}{2}z - b(1 + 4e^{-az})^{-1/2}\sinh^{-1}(\tfrac{1}{2}e^{az/2}) \quad , \tag{4.61}$$

with

$$a = \tfrac{3}{2}\alpha^2 = 2.845\,214\ldots \quad , \tag{4.62}$$

$$b = 3\alpha^7/5\pi\zeta(2\tfrac{1}{2}) = 1.338\,128\ldots \quad . \tag{4.63}$$

For hard-wall conditions the basic expression (4.30) may similarly be truncated at order l^{-1}.

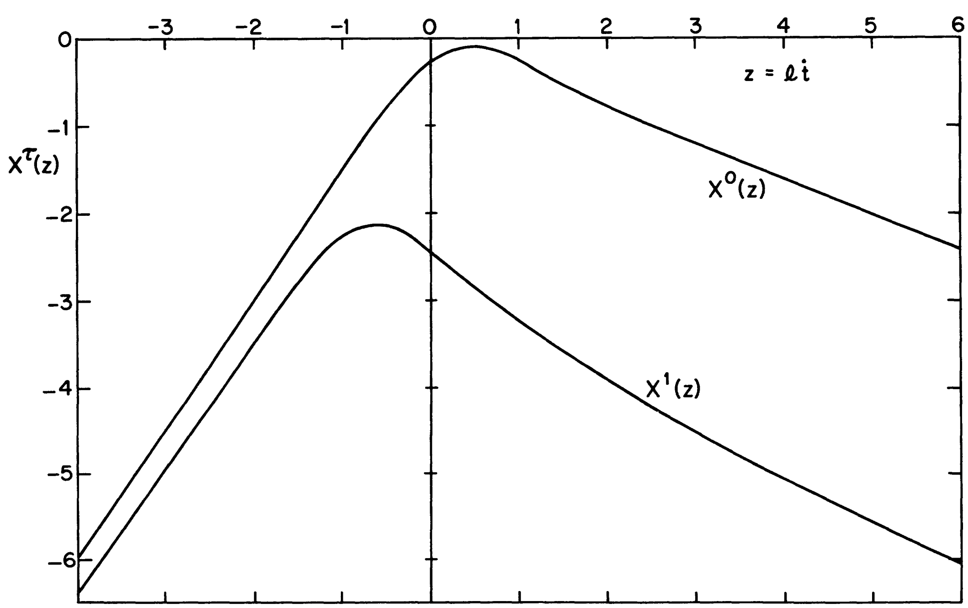

FIG. 4. Scaling functions $X^\tau(z)$ for the specific heat of a two-dimensional Bose film with hard-wall ($\tau = 1$) and periodic ($\tau = 0$) boundary conditions.

However, to obtain a scaled form we must now introduce a shifted temperature deviation[15]

$$\dot{t} = t - \tfrac{2}{3}\alpha^{-2} l^{-1} \ln(4l\pi^{1/2}/\alpha) \ , \tag{4.64}$$

in which case (4.23) becomes

$$\dot{\theta} = \tfrac{3}{2}\alpha^2 l\dot{t} + O(l\dot{t}^2) \ . \tag{4.65}$$

The expression (4.30) may then be written in the more complex scaled form

$$C_V^1(T,l) = C_{Vc}[1 + \alpha^{-2} l^{-1} \ln(4l\pi^{1/2}/\alpha) + l^{-1} X^1(l\dot{t}) + O(l^{-2})] \ . \tag{4.66}$$

On introducing (4.31), (4.28), and (4.26) the scaling function $X^1(z)$ may be written parametrically as

$$X^1(z) = \tfrac{3}{2}z - c^{\times} - \tfrac{1}{2} b u^2 (u \coth u - 1)^{-1} \ , \quad z = a^{-1}\ln(\sinh u/u) \ , \tag{4.67}$$

where

$$c^{\times} = 2\pi^2(\tfrac{2}{3}a)^{1/2}/45\zeta(2\tfrac{1}{2}) = 0.450\,341\ldots \ , \tag{4.68}$$

and a and b are given in (4.62) and (4.63). The scaling functions $X^{\tau}(z)$, which are always negative, are shown graphically in Fig. 4. Somewhat paradoxically, the scaling function for hard-wall conditions exhibits a maximum below $z=0$, i.e., for $\dot{t}<0$, even though the specific-heat maximum lies above T_c. This arises, of course, because of the logarithmic shift[15] in (4.64) which dominates the relation between t and $\dot{t}$ for large l.

Finally, it remains to check that these scaling forms, (4.60) and (4.66), reproduce the bulk behavior, (1.3), in the limit $l\to\infty$, with T fixed near T_c. From the relation $z = l\dot{t}$, we see that the limit $l\to\infty$, with t fixed corresponds to

(i) $z \to -\infty$ if $t<0$,

(ii) $z\to+\infty$ if $t>0$,

in the scaling functions $X^{\tau}(z)$. For periodic boundary conditions, we immediately obtain from (4.61) the asymptotic forms

$$X^0(z) = \tfrac{3}{2}z + O(e^{-|z|}) \ , \qquad z\to-\infty \ ,$$
$$= \tfrac{1}{2}(3-ab)z + O(e^{-z}) \ , \quad z\to+\infty \ . \tag{4.69}$$

Substituting these results in (4.60) yields

$$C_V^0(T,l)/C_{Vc} = 1 + \tfrac{3}{2}t + O(e^{-l|t|}), \qquad l\to\infty, \quad T<T_c \ ,$$
$$= 1 + \tfrac{1}{2}(3-ab)t + O(e^{-lt}), \quad l\to\infty, \quad T>T_c \ . \tag{4.70}$$

From this one easily recovers (1.3). Note the exponentially fast approach to the limiting behavior[3,4,7] alluded to at the end of Sec. III.

For hard-wall boundary conditions the analysis is similar. The asymptotic behavior of $X^1(z)$ as $z\to\infty$ follows directly from (4.67) by considering the limit $u\to\infty$ which yields

$$X^1(z) = \tfrac{1}{2}(3-ab)z - \tfrac{1}{2}b(\ln z) + O(1) \quad \text{as } z\to\infty \ . \tag{4.71}$$

The limit $z\to-\infty$ is slightly more subtle since from (4.67) it follows that $z<0$ corresponds to $u=iv$, $v>0$. The limit $z\to-\infty$ then corresponds to $v\to\pi$ which yields

$$X^1(z) = \tfrac{3}{2}z - c^{\times} + O(e^{-|z|}) \quad \text{as } z\to\infty \ . \tag{4.72}$$

The leading terms in these expansions of $X^1(z)$ are identical to those for $X^0(z)$; hence the bulk behavior, (1.3), is again reproduced. With hard walls, however, the corrections for t fixed are, as expected, of order l^{-1}. Furthermore, on recalling the definition (1.9) of the surface specific heat $C_V^{\times}(T)$, we see that (4.71) and (4.72) imply

$$C_V^{\times}(T)/C_{Vc} \approx -\tfrac{1}{2}c^{\times} \qquad \text{as } T\to T_c - $$
$$\approx \tfrac{1}{4}b\ln(t^{-1}) + O(1) \quad \text{as } T\to T_c + , \tag{4.73}$$

where $c^{\times}$ is defined in (4.68) and b in (4.63). It is easily checked with the aid of (1.1), (3.2), and (4.62) that these asymptotic results are the same as those obtained directly from the evaluation of the surface specific-heat in Sec. III [see (3.23) and (3.26)]. Thus the scaling formulation describes correctly not only the bulk critical behavior, but also the surface terms.

E. Conclusions

This completes our analysis of the specific heat of an ideal Bose film. It seems overly optimistic to expect such an idealized model to be applicable in any detail to films of real helium, as has been suggested in the past by several authors.[8–10] In particular, the simple product $z = lt$, corresponding to $\nu=1$ in (1.4),[3] is unlikely to provide the correct scaling variable, nor is the shift in the (quasi) critical point likely to vary as $(\ln l)/l$ as we have found for the ideal fluid. What is significant, however, is the rather complete verification provided by the ideal system of the predictions of the scaling theory of finite-size effects.[3,4] It is this general theory that one would hope might be applicable to the behavior of real helium films. Indeed, some data[16] already exist which are not inconsistent[4,17] with scaling. A future experimental priority should be accurate measurements which will allow a more detailed evaluation of the scaling theory for real systems, and, in particular, lead to estimates of the true exponent ν for the correlation length and the exponent λ for the shift in critical (or quasicritical) point.[3,4]

ACKNOWLEDGMENTS

The authors would like to thank Professor D. F. Goble for sending some of his unpublished graphical data, which facilitated the comparisons made here. The work was supported by the Advanced Research Projects Agency, through the Materials Science Center at Cornell University, and by the National Science Foundation. One of us (M. N. B.) is grateful to the Commonwealth Scientific and Industrial Research Organization of Australia for the award of an overseas postgraduate studentship.

---

*Present address: Department of Applied Mathematics, Research School of Physical Sciences, Australian National University, Canberra, A.C.T. 2601, Australia.

[1]M. N. Barber and M. E. Fisher, Ann. Phys. (N.Y.) (to be published, 1973).

[2]T. H. Berlin and M. Kac, Phys. Rev. **86**, 821 (1952).

[3]M. E. Fisher, in *Critical Phenomena, Proceedings of the Enrico Fermi Summer School, Varenna, Italy, 1970, Course No. 51* (Academic, New York, 1971); for other aspects of critical phenomena, particularly exponent definitions, etc., see M. E. Fisher, Rep. Prog. Phys. **30**, 615 (1967).

[4]M. E. Fisher and M. N. Barber, Phys. Rev. Lett. **28**, 1516 (1972).

[5]F. London, *Superfluids* (Dover, New York, 1954), Vol. II.

[6]J. D. Gunton and M. J. Buckingham, Phys. Rev. **166**, 152 (1968); see also M. Cooper and M. S. Green, Phys. Rev. **176**, 302 (1968).

[7]For a preliminary report see M. N. Barber and M. E. Fisher, in Proceedings of the I.U.P.A.P. Conference on Statistical Mechanics, Chicago, April, 1971 (unpublished); full details have been submitted for publication by M. N. Barber.

[8]M. F. M. Osborne, Phys. Rev. **76**, 396 (1949); J. M. Ziman, Philos. Mag. **44**, 548 (1953); M. Toda and F. Takano, J. Phys. Soc. Jap. **9**, 14 (1954); A. D. Singh and R. K. Pathria, Prog. Theor. Phys. **24**, 229 (1960); D. L. Mills, Phys. Rev. **134**, A306 (1964); B. M. Khorana and D. H. Douglass, Phys. Rev. **138**, A35 (1965); D. A. Krueger, Phys. Rev. Lett. **19**, 563 (1967); Phys. Rev. **172**, 211 (1968).

[9]D. F. Goble and L. E. H. Trainor, Can. J. Phys. **44**, 27 (1966).

[10]D. F. Goble and L. E. H. Trainor, Phys. Rev. **157**, 167 (1967); Can. J. Phys. **46**, 1867 (1968).

[11]R. K. Pathria, Phys. Rev. A **5**, 1451 (1972).

[12]F. London, in Ref. 5, p. 203.

[13]*Higher Transcendental Functions*, edited by A. Erdélyi (McGraw-Hill, New York, 1953), Vol. I, Chap. 1.

[14]M. E. Fisher and M. N. Barber, Arch. Ration. Mech. Anal. **47**, 205 (1972).

[15]Note that the coefficient $4\sqrt{\pi}/\alpha$ in the argument of the logarithm is essentially arbitrary; it could be altered merely at the cost of shifting the scaled variable $z = lt$ entering (4.67), by a corresponding amount. In this way the maximum in $X^1(z)$ (see Fig. 4) could be shifted to lie at positive (or zero) z.

[16]D. F. Brewer, J. Low Temp. Phys. **3**, 205 (1970).

[17]M. A. Moore, Phys. Lett. A **37**, 345 (1971).